J. Fluid Mech. (1969), *vol.* 39, *part* 1, *pp.* 97–115
Printed in Great Britain

Lateral motion of a slender body between two parallel walls

By J. N. NEWMAN

Department of Naval Architecture and Marine Engineering
Massachusetts Institute of Technology

(Received 26 December 1968 and in revised form 4 June 1969)

The method of matched asymptotic expansions is used to determine the lateral flow of an ideal fluid past a slender body, when the flow is constrained by a pair of closely spaced walls parallel to the long axis of the body. In the absence of walls, the flow field would be nearly two-dimensional in the cross-flow plane normal to the body axis, but the walls introduce an effective blockage in the cross-flow plane, which causes the flow field to become three-dimensional. Part of the flow is diverted around the body ends, and part flows past the body in the inner cross-flow plane with a reduced 'inner stream velocity'. An integro-differential equation of identical form to Prandtl's lifting-line equation is derived for the determination of this unknown inner stream velocity in the cross-flow plane. Approximate solutions are applied to determine the added mass and moment of inertia for accelerated body motions and the lift force and moment acting on a wing of low aspect ratio. It is found that the walls generally increase these forces and moments, but that the effect is significant only when the clearance between the body and the walls is very small.

1. Introduction

When a rigid slender body moves through an infinite ideal fluid, it is known that there exist significant three-dimensional effects, involving interactions between adjacent sections of the body, only when it moves in longitudinal translation parallel to its long axis. For lateral translation, in directions normal to the body axis, as well as for rotational motions of the body, the resulting flow is locally two-dimensional and confined to the 'cross-flow' plane at each section without significant interaction between adjacent sections of the body (cf. Thwaites 1960). Moreover, it is well known that the lifting problem of a wing of small aspect ratio can be analyzed in the same manner as the lateral translation of a non-lifting slender body, so that here, too, the flow is locally two-dimensional in the cross-flow plane.

Generally speaking, these results are not qualitatively changed if the body moves parallel to a single wall, or an infinite plane boundary of the fluid, and the wall will serve only to introduce a perturbation of the original flow. As an example of this type of problem, Newman (1965) has treated the longitudinal translation of a slender body of revolution, moving near an infinite wall; the

wall introduces an attractive force and moment which act on the body, but the qualitative features of the flow do not change as a result of the proximity of the wall, and the original formulation of the slender-body approximation does not require fundamental modification. The lateral motion of a slender body of revolution near a single wall is less amenable to analysis, since the exact solution in the cross-flow plane can no longer be obtained in closed form, but one can expect the cross-flow approximation to remain valid, and the problem is essentially amenable to a two-dimensional strip-theory approach.

If the body is situated between *two* parallel walls, with its long axis parallel to these boundaries, the flow field is more significantly affected. Indeed, it is clear that the far-field flow must now be two-dimensional, in planes parallel to the walls, but in fact, for longitudinal motion, this serves as a slight simplification. The closely related problem of longitudinal steady motion of a ship in shallow water has been treated by Tuck (1966). The case of lateral motion of the body between two parallel walls involves a more significant wall effect, for now the original cross-flow hypothesis breaks down and the flow must be considered to be three-dimensional, with interaction between the different sections of the body. As an extreme example, if the gaps between the body and the walls are closed, then the fluid must pass entirely around the ends of the body, and this flow field will be two-dimensional, not in the cross-flow plane, but in planes parallel to the walls, where the body will appear as a thin barrier at normal incidence.

The lateral motion problem is of practical importance in attempting to analyze ship manoeuvres in shallow water, and will be considered here. There is increasing interest in shallow-water effects on ships, because of the large draft of super-tankers, which may typically draw 20 m, and are required to navigate for extended periods in water depths of comparable magnitude. If the ship's speed is not large (more precisely, if the Froude numbers based on the ship length and fluid depth are both small compared to unity), free-surface effects can be neglected, so that reflexion about the free surface results in an equivalent problem involving the flow past a submerged body between two horizontal rigid boundaries. This problem may also have aerodynamic applications, as it is essentially that of a wing of small aspect ratio, separated by small gaps from two infinite boundaries, or from an infinite lateral array of identical bodies.

The transition from a pure cross-flow to one involving three-dimensional motion, and ultimately to one where the flow is two-dimensional in a longitudinal plane, is not at first glance amenable to the usual slender-body approximation. It will be seen, however, that the method of matched asymptotic expansions (cf. Van Dyke 1964) leads to a solution which is related to Prandtl's lifting-line theory for wings of large aspect ratio. The inner flow, close to the body, is indeed a cross-flow in the usual sense, but with a reduced stream velocity incident upon each section of the body due to the blockage effect. The outer solution appears as a two-dimensional flow in planes parallel to the wall, with the undiminished transverse stream velocity incident from infinity and the body reduced to a line or cut normal to the flow, and with part of the flow passing around the body and some of it passing 'through' the body. Matching of these two solutions

results in a unique determination of the reduced inner stream velocity, and hence of all the essential details of the flow field.

Throughout the analysis the fluid is considered as inviscid and incompressible. Viscous effects may affect the validity of the results, due to separation of the flow around the body and also to the existence of a boundary layer between the body and the walls. The former is a familiar problem in analyzing the lateral motions of slender bodies and will not be discussed here. Boundary layer effects would be serious if the body were fixed and the fluid was in motion relative to the infinite walls,† but in practice the body will be moving instead, into a fluid which is at rest at infinity, so that the boundary layer should be relatively thin.

In §§2–4 we shall treat, by the method of matched expansions, the simplest case of uniform lateral translation. The resulting solution is used in §5 to yield the added-mass coefficient for the body. More general lateral motions are considered in §6, with application to the added moment of inertia associated with rigid-body rotation. In §7, we consider the lifting problem, where the body is moving in the longitudinal direction, but with a small angle of attack about an axis normal to the walls, so that a lift force is developed parallel to the walls. In §8, the added mass and moment of inertia, and the lift force and moment, are determined for a rectangular flat plate, and comparison is made with recent experiments on a yawed ship model in shallow water.

2. Problem statement

Cartesian co-ordinates are employed, the x axis coinciding with the longitudinal body axis. Two infinite walls are located parallel to the x–y plane, with one on each side of the body. It is not essential to assume that these planes are symmetrically situated with respect to the x–y plane, but the simple examples considered here will be symmetrical in this sense. Thus, the fluid occupies the domain $-\frac{1}{2}a < z < \frac{1}{2}a$; except for the interior of the body. For convenience, the length scale is chosen such that the body length is equal to two, with the ends situated at the points $(\pm 1, 0, 0)$ (see figure 1). Slenderness of the body implies not only that its transverse dimensions are small, or that every point on the body surface lies within a distance ϵ of the x axis, with $\epsilon \ll 1$, but also that the longitudinal distances, over which changes in body shape occur, are $O(1)$. In order for the walls to significantly affect the cross-flow past the body, it is implicit that $a = O(\epsilon)$, although the final results of our theory appear to be valid without this restriction, reducing for larger wall separation to the classical slender-body results. Finally, for distances from the body which are large compared to its length, the flow field appears as a uniform stream of velocity V, moving parallel to the y axis, so that the velocity potential must satisfy the condition

$$\partial\phi/\partial y \cong V, \tag{2.1}$$

or, after integrating with respect to y and setting the constant of integration equal to zero,

$$\phi(x, y, z) \cong Vy, \quad \text{for} \quad y \gg 1. \tag{2.2}$$

† In this case the motion would resemble that in a Hele–Shaw cell.

3. The inner expansion

The inner region of the flow is that region where y is small compared to the length. Here, except for a longitudinal velocity component which depends only on x, the flow is confined to the cross-flow plane at each section by virtue

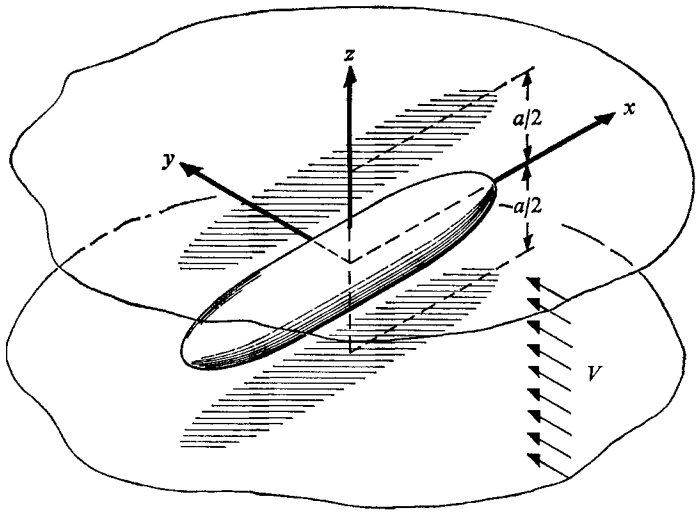

FIGURE 1. The co-ordinate system and flow geometry. The planes $z = \pm \frac{1}{2}a$ are rigid infinite walls, and the length scale is chosen such that the body ends are at $x = \pm 1$.

of the usual inner (two-dimensional) expansion of Laplace's equation, and will appear as shown in figure 2. In the inner region, the lateral stream velocity incident upon the body will be denoted by $U(x)$. In general, this inner stream velocity will be reduced, from its outer value V, due to the partial diversion of the outer flow around the body ends. Thus, in the inner region, we impose the limiting condition

$$\partial\phi/\partial y \cong U, \tag{3.1}$$

or

$$\phi \cong U(y \pm C) \quad \text{for} \quad \epsilon \ll |y| \ll 1, \tag{3.2}$$

where the $\pm$ corresponds respectively to $y \gtrless 0$. Here C is a parameter, which can be regarded as a constant of integration, and will generally vary along the body length, so that $C = C(x)$. (Variations of $U(x)$ and $C(x)$ are assumed to be small, over distances $O(\epsilon)$.) It is essential to include the parameter C in (3.2) since, in general, the potential at $x = \pm\infty$ will differ by a constant in any two-dimensional flow of the type considered here.† This point has been discussed in a

† The situation in §2 differs, and the constant of integration in (2.2) could be deleted, essentially because, at infinity *in the outer region*, (2.2) must hold for large values of the polar radius $r = (x^2+y^2)^{\frac{1}{2}}$ at all polar angles $\tan^{-1} y/x$, so there can be no jump as in (3.2). It may be noted that, in both (2.2) and (3.2), the constant of integration has been chosen so that these potentials are odd functions of y; this is a premature, but trivial, application of the matching principle.

similar context by Tuck (private communication), in connexion with the inner expansion of a water-wave scattering problem.

The 'blockage parameter' C can be determined from the conformal-mapping function of the given flow geometry, or alternatively from direct solution of the potential problem. The simplest example of the latter is the flow past an infinite

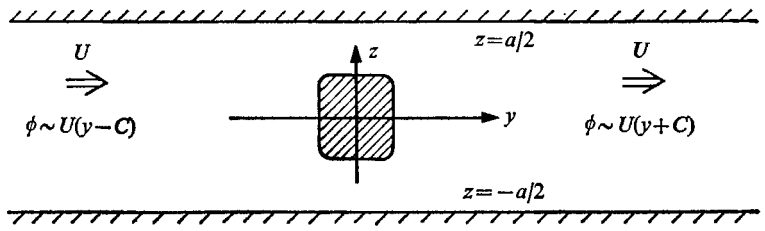

FIGURE 2. The inner flow region.

array of dipoles, directed opposite to the stream, and equally spaced along a line normal to this direction, so that to a first approximation the dipoles represent the normal flow past an infinite cascade of circles. By the method of images, this problem is then equivalent to the flow past a single nearly-circular section situated midway between two parallel walls. From Lamb (1932, §64) it follows directly that

$$C \cong S/a, \tag{3.3}$$

where S is the cross-sectional area of the circle. Lamb notes that this approximation introduces a negligible error provided the diameter is less than half the wall separation a.

More generally, the inner flow can be likened to the flow past a cascade of two-dimensional non-lifting bodies, and information can be obtained from Sedov (1950, chapter III). In particular, Sedov notes (equation 8.6) that the constant C can be related to the added-mass coefficient of the profile, in accordance with the equation

$$\lambda_{yy} = -\rho S + 2\rho a C. \tag{3.4}$$

Here λ_{yy} is the coefficient of added mass, or the hydrodynamic force acting to resist a unit acceleration of the body in the direction of the y axis, ρ is the fluid density, and S denotes the area circumscribed by the profile. Sedov gives values of the coefficient λ_{yy} for various cascaded profiles, including a flat plate of width d normal to the stream, and a limited class of rectangles. For the flat plate

$$\lambda_{yy} = -2\rho \frac{a^2}{\pi} \log \cos \frac{\pi d}{2a}, \tag{3.5}$$

so that in this case the constant C is given by the relation

$$C = -\frac{a}{\pi} \log \cos \frac{\pi d}{2a}. \tag{3.6}$$

No further analysis of the inner flow is required, and we shall assume that for the body sections under consideration sufficient information exists regarding the parameter C.

4. The outer flow and the matching process

For transverse distances $y = O(1)$, the body appears as a cut of negligible thickness on the x axis, and local flow conditions, which existed in the inner solution, are absorbed entirely into the singular behaviour on this cut. Moreover, as the perturbation parameter ϵ tends to zero, recalling that the wall separation distance $a = O(\epsilon)$, the outer flow will be confined increasingly to planes parallel to the walls, so that to a first approximation in the slenderness parameter the outer flow appears as a two-dimensional field, in the x–y plane. The resulting outer flow is as shown in figure 3; it is clear that this is physically similar to the flow past a porous flat plate at normal incidence, with the flux through the plate representing the flux past the body in the cross-flow plane of the inner solution,

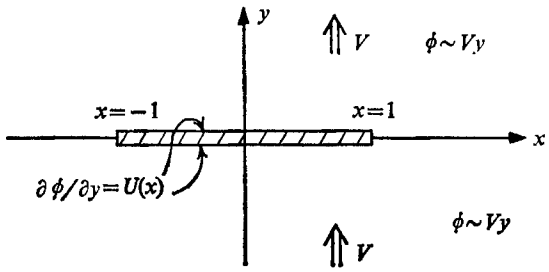

FIGURE 3. The outer flow region.

and the flux past the body ends representing the tendency for some of the fluid to pass around the ends due to the blockage in the cross-flow plane. For the sake of generality, we shall take the normal velocity on the cut to be

$$\frac{\partial \phi}{\partial y} = v_0(x) \quad \text{on} \quad -1 < x < 1, \tag{4.1}$$

with $v_0(x)$ an unknown which is to be subsequently determined by the matching procedure. (From continuity considerations we might anticipate that $v_0 = U$, and this will be confirmed.)

The solution of the above-stated problem is readily obtained from standard Hilbert transform techniques. Thus the complex velocity,

$$f(z) = u - iv,$$

is an analytic function of the complex variable $z = x + iy$, subject to the conditions

$$\mathrm{Im} f(x, \pm 0) = -v_0(x) \quad \text{on} \quad -1 < x < 1, \tag{4.2}$$

and

$$f(z) \cong -iV \quad \text{for} \quad |z| \to \infty. \tag{4.3}$$

It is also necessary to impose the requirement that

$$\mathrm{Re} f(x, 0) = 0 \quad \text{for} \quad |x| > 1, \tag{4.4}$$

which follows from the symmetry of the outer flow about the x axis and, in addition, the singularity condition that

$$(z^2 - 1) f(z) \to 0 \quad \text{for} \quad z \to \pm 1. \tag{4.5}$$

The last condition is common and occurs, e.g. in dealing with the leading-edge singularity of a thin aerofoil; essentially (4.5) ensures that the velocity field contains no stronger singularities at the ends of the cut than the square-root infinities, which are familiar in the case of the flow incident upon an impermeable flat plate at normal incidence.

We follow the usual method for solution of such problems (cf. Muskhelishvili 1946): the function $f(z)\,(1-z^2)^{\frac{1}{2}}$ is analytic in the cut z plane and, from (4.2) and (4.4), its imaginary part is specified on the entire real axis. Therefore, this function can be determined from Cauchy's integral theorem, for all values of z outside the cut, by the integral

$$f(z)\,(1-z^2)^{\frac{1}{2}} = -\frac{1}{\pi}\int_{-1}^{1} \frac{v_0(\xi)(1-\xi^2)^{\frac{1}{2}}}{\xi - z}\,d\xi + P(z), \tag{4.6}$$

where $P(z)$ is an arbitrary polynomial with real coefficients, which denotes the homogeneous solution of (4.2) and (4.4).

Dividing both sides of (4.6) by the square-root function and imposing the condition at infinity from (4.3) gives:

$$f(z) = u - iv = -\frac{1}{\pi(1-z^2)^{\frac{1}{2}}}\int_{-1}^{1} \frac{v_0(\xi)(1-\xi^2)^{\frac{1}{2}}}{\xi - z}\,d\xi + \frac{Vz + P(0)}{(1-z^2)^{\frac{1}{2}}}. \tag{4.7}$$

In particular, for points close to the cut,

$$u(x, \pm 0) = \mp\frac{1}{\pi(1-x^2)^{\frac{1}{2}}}\int\!\!\!\!\!\!-_{-1}^{1} \frac{v_0(\xi)(1-\xi^2)^{\frac{1}{2}}}{\xi - x}\,d\xi \mp \frac{Vx + P(0)}{(1-x^2)^{\frac{1}{2}}}, \tag{4.8}$$

and

$$v(x, \pm 0) = v_0(x). \tag{4.9}$$

Here $\int\!\!\!\!\!\!-$ denotes the Cauchy principal-value integral.

Matching of the outer flow with the inner solution implies that (4.8) and (4.9) must be matched with the asymptotic values of the same velocity components at large distances from the body section in the inner flow where, from (3.2),

$$\frac{\partial \phi}{\partial x} \cong U'(x)y \pm (UC)' \quad \text{for} \quad \epsilon \ll y \ll 1, \tag{4.10}$$

and

$$\partial\phi/\partial y \cong U(x). \tag{4.11}$$

In (4.10), and hereafter, a prime denotes the derivative with respect to x. Equating (4.9) and (4.11) gives the anticipated result

$$v_0(x) = U(x). \tag{4.12}$$

Matching (4.8) and (4.10) then gives the integral equation

$$[U(x)C(x)]' = -\frac{1}{\pi(1-x^2)^{\frac{1}{2}}}\int\!\!\!\!\!\!-_{-1}^{1} \frac{U(\xi)(1-\xi^2)^{\frac{1}{2}}}{\xi - x}\,d\xi - \frac{Vx + P(0)}{(1-x^2)^{\frac{1}{2}}}, \tag{4.13}$$

for $-1 < x < 1$.

Equation (4.13) is the ultimate result of the matching process. It is a singular integro-differential equation for the unknown inner stream velocity $U(x)$, assuming that the body velocity V is given and the blockage parameter $C(x)$ has been determined from the geometry of the inner region. It is clear that the

only influence of the body geometry and of the wall separation on the outer flow, and on the inner stream velocity, is *via* this parameter.

In order to determine the constant $P(0)$, a suitable end-condition must be imposed. For a body with non-square ends, or one for which the body-radius vanishes at the ends, $C(\pm 1) = 0$, since the blockage parameter must be zero if there is no finite body in the inner region. If the body ends are square (a situation in which the slender-body approximation must be regarded with caution!), it is physically apparent that the flow at the ends will be completely diverted by blockage, so that in this case $U(\pm 1) = 0$. Thus, in general, the product UC should satisfy the condition

$$U(x)C(x) = 0 \quad \text{at} \quad x = \pm 1. \tag{4.14}$$

To relate this condition to $P(0)$, (4.13) will be integrated, with respect to x, to give the Fredholm equation,

$$U(x)C(x) - U(1)C(1) = -\frac{1}{\pi}\int_{-1}^{1} U(\xi)K(x,\xi)\,d\xi + V(1-x^2)^{\frac{1}{2}} - P(0)(\tfrac{1}{2}\pi + \sin^{-1}x). \tag{4.15}$$

Here $K(x, \xi)$ is the symmetric kernel defined by

$$K(x,\xi) = \oint_{-1}^{x} \frac{(1-\xi^2)^{\frac{1}{2}}\,dx}{(1-x^2)^{\frac{1}{2}}(\xi - x)} = \tfrac{1}{2}\log\left[\frac{1-\xi x + (1-\xi^2)^{\frac{1}{2}}(1-x^2)^{\frac{1}{2}}}{1-\xi x - (1-\xi^2)^{\frac{1}{2}}(1-x^2)^{\frac{1}{2}}}\right]. \tag{4.16}$$

Since this kernel vanishes when $x = \pm 1$, it follows that the constant $P(0)$ must be equal to zero, in order to satisfy (4.14). Thus we obtain finally the Fredholm equation

$$U(x)C(x) = -\frac{1}{\pi}\int_{-1}^{1} U(\xi)K(x,\xi)\,d\xi + V(1-x^2)^{\frac{1}{2}}. \tag{4.17}$$

For sufficiently large values of C, (4.17) can be solved by iteration, and the first stage in such a scheme is clearly

$$U(x) \cong (1-x^2)^{\frac{1}{2}}(V/C). \tag{4.18}$$

This approximation is relevant in the case where the separation of the walls from the body is very small. The opposite extreme, where the walls are far away from the body, corresponds to the limit where C vanishes, and we then obtain the correct physical limit $U = V$.

An alternative scheme is to operate on (4.13) with the inversion operator for Cauchy integral equations, so that the unknown U appears only as a free term and the integral involves the derivative $(UC)'$. This approach is convenient, because the resulting integral equation is identical to Prandtl's lifting-line equation, and well-known solutions can be borrowed for the present problem. Thus, we shall operate on both sides of (4.13) with the inversion operator

$$\oint_{-1}^{1} \frac{dx}{x-t}(\ ),$$

and use the Poincaré–Bertrand formula (Muskhelishvili 1946) to evaluate the resulting double integral. In this manner, we obtain from (4.13) the alternative integro-differential equation

$$U(t) = \frac{1}{\pi} \int_{-1}^{1} \frac{(UC)'\, dx}{x-t} + V. \tag{4.19}$$

The form of (4.19) is identical with Prandtl's classical lifting-line equation (cf. Thwaites 1960). The unknown inner stream velocity U, along with the known outer stream velocity V and the blockage parameter C, can be related directly to the aerodynamic problem of a wing of large aspect ratio, in terms of the substitutions

$$U = C_L/2\pi, \tag{4.20}$$

$$V = \alpha, \tag{4.21}$$

and

$$C(x) = \pi c(x)/4. \tag{4.22}$$

Here C_L is the spanwise local lift-coefficient of the wing, α is the angle of attack, and $c(x)$ is the local chord. By analogy with the non-dimensional co-ordinates of our problem, the aerofoil must occupy the cut $|x| < 1$ and is, therefore, of span equal to two. For the case of infinite aspect ratio, we recover the limiting result that $U = V$, since for a two-dimensional flat aerofoil $C_L = 2\pi\alpha$. Moreover, the requirement that the wing loading vanish at the tips corresponds in our problem to the vanishing of UC at the ends of the body.

Two special cases will now be discussed. First, we consider the simple case of an elliptic 'planform', where the blockage parameter C is

$$C(x) = C(0)(1-x^2)^{\frac{1}{2}}. \tag{4.23}$$

Then the aerodynamic loading is also elliptical, and the solution for the 'flux-defect-ratio' is the constant

$$\frac{U}{V} = \frac{1}{1+C(0)}. \tag{4.24}$$

(Note that this special case is consistent with the 'low aspect ratio' limit of small wall-separation, or large C, as given by (4.18).) If we employ Lamb's approximation (3.3) for nearly circular sections, it is apparent that (4.23) corresponds to a body of revolution with an elliptic distribution of sectional area, or a body which is somewhat more blunt than a spheroid.

As our second example we consider the analogue of a rectangular wing, or $C(x) =$ constant, corresponding to a cylindrical body with square ends. In this case, the complete solution requires a numerical procedure, such as the use of a Glauert trigonometric series. However, the departure of the load distribution from an elliptic form is quite small, and this difference vanishes in the limit of small aspect ratio, so that for the present purposes there seems little point in considering any but the first term in the Glauert series. Thus, with $x = \cos\theta$, we assume that U/V is of the form $A_1 \sin\theta$. Determination of the constant A_1, from the requirement that the average of the flux-defect-ratio be equal to one when $C \to 0$ then leads us to the approximate solution,

$$\frac{U}{V} = \frac{\sin\theta}{C+\frac{1}{4}\pi} = \frac{(1-x^2)^{\frac{1}{2}}}{C+\frac{1}{4}\pi}. \tag{4.25}$$

5. The added-mass coefficient

As an application of the preceding results, we shall determine the added mass of a slender body in lateral acceleration, including the effects of the walls. In order to distinguish from the two-dimensional coefficient of added mass λ_{yy}, which was introduced in the discussion of the inner flow, we shall denote the total added-mass coefficient of the three-dimensional flow by M_{yy}, and the corresponding local added-mass coefficient of each section, in the three-dimensional flow, by m_{yy}. It is also convenient to define the body volume as

$$\mathcal{V} = \int_{-1}^{1} S\,dx. \tag{5.1}$$

The three-dimensional added-mass coefficient can be determined by application of a stripwise analysis, integrating the local coefficient of each cross-section of the body over its length. Thus

$$M_{yy} = \int_{-1}^{1} m_{yy}\,dx. \tag{5.2}$$

The desired sectional force coefficient m_{yy} differs from the two-dimensional coefficient λ_{yy} due to the three-dimensional effects on the flow field, but it can be found, by analogy with (3.4), from the jump in the inner velocity potential which occurs between the two infinities of the inner solution. For the purely two-dimensional flow, the velocity U corresponded to the lateral velocity of the body, and in three dimensions the velocity of the body is V, relative to the fluid fixed at infinity. Noting that the ratio of the two accelerations, $\dot{U}/\dot{V}$, equals the ratio of the two velocities U/V, it follows that (3.4) must be modified by this ratio to determine the three-dimensional sectional added-mass force, or

$$m_{yy} = -\rho S + 2\rho a C U/V. \tag{5.3}$$

Integration then yields

$$M_{yy} = -\rho\mathcal{V} + 2\rho a \int_{-1}^{1} (UC/V)\,dx. \tag{5.4}$$

For the case C = constant, the approximation (4.25) can then be employed, and it follows that

$$M_{yy} = -\rho\mathcal{V} + \frac{4\rho a C}{1 + 4C/\pi}. \tag{5.5}$$

For small values of the blockage parameter C, this result is equivalent to the direct stripwise application of the two-dimensional added mass from (3.4). The opposite limit, $C \to \infty$, corresponds to the case where the body is in contact with the walls, so that the flow is diverted completely around the ends. In this limit we have

$$M_{yy} = -\rho\mathcal{V} + \pi\rho a, \tag{5.6}$$

which is the (two-dimensional) virtual mass of the cut on the x axis, of length 2, multiplied by the width a.

An alternative method for determining the value of the integral in (5.4) is in terms of a suitable variational integral. For this purpose, we first integrate (4.17) to get the relation,

$$I = \int (UC/V)\,dx = \tfrac{1}{2}\pi - \int_{-1}^{1} (U/V)\sqrt{(1-x^2)}\,dx. \tag{5.7}$$

We shall denote the last integral by J, and use (4.17) to derive a variational principle for J, following the analogous procedure outlined for water-wave scattering by Miles (1967). Multiplying both sides of (4.17) by (U/V^2), and integrating once again, leads to the equation,

$$J = \int_{-1}^{1} (U/V)(1-x^2)^{\frac{1}{2}}\,dx = \int_{-1}^{1} (CU^2/V^2)\,dx + \frac{1}{\pi}\int_{-1}^{1} (U/V)\,dx \int_{-1}^{1} (U/V)K(x,\xi)\,d\xi. \tag{5.8}$$

Dividing the last result into the square of the first, it follows that

$$J = \frac{\left[\int_{-1}^{1} (U/V)(1-x^2)^{\frac{1}{2}}\,dx\right]^2}{\int_{-1}^{1} (CU^2/V^2)\,dx + \frac{1}{\pi}\int_{-1}^{1} (U/V)\,dx \int_{-1}^{1} (U/V)K(x,\xi)\,d\xi}. \tag{5.9}$$

This equation can now be used to determine, for a given approximation of the flux-defect ratio U/V, the added-mass coefficient. Its chief virtues are its invariance to changes in scale of the trial function U/V, and the fact that it is stationary with respect to first-order perturbations of the trial function about the exact solution of (4.17). An indication of its accuracy is the fact that, for C = constant, the very crude approximation $U/V = 1$ yields from (5.9) the added-mass coefficient (5.5), which was obtained directly from the more accurate approximation for U/V given by (4.25). If (4.25) is now used in conjunction with (5.9), the resulting added-mass coefficient is found, after evaluating the necessary integrals, in the form,

$$M_{yy} = -\rho\mathscr{V} + 2\pi\rho a \frac{\frac{2}{3}\pi C + \frac{3}{4} - \frac{16}{9} + \frac{7}{8}\zeta(3)}{\frac{4}{3}\pi C + \frac{3}{2} + \frac{7}{4}\zeta(3)},$$

$$\doteqdot -\rho\mathscr{V} + 2\pi\rho a \frac{2{\cdot}094C + 0{\cdot}024}{4{\cdot}189C + 3{\cdot}604}. \tag{5.10}$$

Here $\zeta(3)$ denotes the Riemann zeta-function of argument 3. Comparing this new approximation with (5.5), it is seen that the limiting result $C \to \infty$ is unchanged, but for very small values of the blockage parameter C, the new result is less accurate. Comparison with Glauert's (1948) numerical solution for a rectangular wing reveals that both of our approximations are equally in error, by about 4 % for the integral I, when $C = \frac{1}{7}$, but for $C = 1$ the error in the first approximation (5.5) is unchanged, while the second approximation (5.10) agrees with Glauert's results to three significant figures.

6. Extension to other body motions

The preceding analysis can be generalized to include lateral velocities of the body which are of the form $V(x,t)$. If V is independent of x, the translational motion of §§2–5 results, whereas if V is linear in x, one has the case of rotational motion about the z axis. Higher-order modes of elastic vibration can likewise be considered, although the slender-body assumption requires that $\partial V/\partial x = O(1)$ with respect to ϵ.

In order to derive integral equations for the more general case, the inner flow region may be analyzed in a moving co-ordinate system, which is fixed locally with respect to the body section, so that in this reference frame the body profile is fixed, and the stream velocity at large distances in the inner expansion is $U-V$. The outer velocity field is analyzed in a fixed co-ordinate system, with the requirement that the velocity vanish at infinity, and the matching conditions are then unchanged from (4.10) and (4.11). Proceeding in this manner, the 'lifting-line' equation (4.19) results without modification, and the aerodynamic analogue is a twisted wing, with spanwise variation of the angle of attack, $\alpha = V(x)$. The Fredholm equation (4.17) must be modified, for general $V(x)$, and assumes the form

$$U(x)C(x) = \frac{1}{\pi}\int_{-1}^{1} [V(\xi) - U(\xi)]K(x,\xi)\,d\xi \quad (-1 \leqslant x \leqslant 1), \tag{6.1}$$

where the kernel $K(x,\xi)$ remains as given by (4.16).

For angular rotation about the z axis, we substitute $V(x,t) = \dot{\theta}x$, where $\dot{\theta}$ denotes the angular velocity, and obtain from (6.1) the integral equation

$$U(x)C(x) = -\frac{1}{\pi}\int_{-1}^{1} U(\xi)K(x,\xi)\,d\xi + \tfrac{1}{2}\dot{\theta}x(1-x^2)^{\frac{1}{2}}. \tag{6.2}$$

For large values of the blockage parameter $C(x)$, the first approximation to the function U is

$$U(x) \cong (\dot{\theta}/2C)x(1-x^2)^{\frac{1}{2}}. \tag{6.3}$$

The coefficient of added moment of inertia can be determined in an analogous manner to the added-mass coefficient. The coefficient of the added moment is

$$I_{zz} = -\rho\int_{-1}^{1} x^2 S(x)\,dx + 2\rho a\int_{-1}^{1} (UC/\dot{\theta})x\,dx, \tag{6.4}$$

where the first term represents the moment of inertia of the displaced fluid. To determine the second integral in (6.4) from a variational method, we first multiply (6.2) by $x/\dot{\theta}$ and integrate, to obtain the relation

$$I_{zz} = -\rho\int_{-1}^{1} x^2 S(x)\,dx + \pi\rho a/8 - \rho a\int_{-1}^{1} (U/\dot{\theta})x(1-x^2)^{\frac{1}{2}}\,dx. \tag{6.5}$$

A quadratic form for the last integral can be obtained, by first multiplying (6.2) by $U/\dot{\theta}$ and then integrating, as in the analogous development of (5.9). In this manner it follows that

$$\int_{-1}^{1} (U/\dot{\theta})x(1-x^2)^{\frac{1}{2}}\,dx = \frac{\left[\int_{-1}^{1} U(x)x(1-x^2)^{\frac{1}{2}}\,dx\right]^2}{2\int_{-1}^{1} U^2(x)C(x)\,dx + \frac{2}{\pi}\int_{-1}^{1} U(x)\int_{-1}^{1} U(\xi)K(x,\xi)\,d\xi\,dx}. \tag{6.6}$$

We shall apply (6.5) and (6.6) to the determination of the added moment of inertia for the cylindrical case C = constant. As a first approximation we set $U/\dot{\theta} = x$, and after performing the necessary integrations it follows that

$$I_{zz} \cong -\int x^2 S(x)\,dx + \frac{4\rho a C}{(32/\pi)C+3}. \tag{6.7}$$

To improve upon this approximation, we can use (6.3) in (6.6), and it then follows that

$$I_{zz} = -\rho \int x^2 S(x)\,dx + \rho a \frac{\frac{1}{2}\pi C + \frac{1}{45}}{4C + \frac{40}{9}\pi}. \tag{6.8}$$

Equations (6.7) and (6.8) represent approximations to the added moment of inertia which are analogous to the corresponding results (5.5) and (5.10) obtained for the lateral added-mass coefficient. We can assume that (6.7) will be more accurate for small values of C, and that (6.8) will afford a better approximation for large values of C. For $C > 0{\cdot}1$, the quotients of (6.7) and (6.8) differ by less then 5 %, which suggests that (6.7) is a satisfactory approximation for all values of the blockage parameter C.

7. Application to lifting surfaces of small aspect ratio

The analysis of §§2–4 can also be applied to the problem of a slender lifting surface. If the incident stream is parallel to the two walls, and the body is oriented at a small angle of attack about an axis normal to the walls, the walls will appear as partial end-plates which, in effect, increase the aspect ratio of the lifting surface. Indeed, in the limit where the walls are in contact with the tips of the (rectangular) wing, the problem is purely two-dimensional whereas, in the opposite extreme of large-wall separation, the problem should reduce to its conventional low-aspect-ratio form.

We assume that the body contains a sharp trailing edge, of finite width and situated at $x = 1$, $y = 0$. We also assume, in the usual manner of conventional low-aspect-ratio wing theory, that the leading edge is pointed and situated at $x = -1$, $y = z = 0$. However, the final results for the lift force and moment appear to be valid for a leading edge of finite width; and, in particular, we shall apply them to the case of a rectangular planform.

In order to preserve the previous notation for the lateral stream velocity V, we take the incident stream to be the vector $(1, V, 0)$, thus implying that a suitable scale has been chosen, such that the magnitude of the free steam velocity is unity to first order, and the angle of attack is V, which must be small compared with one. After subtracting off the longitudinal component of the stream velocity $(1, 0, 0)$, and symmetrical-flow thickness effects (if any), the problem reduces to one involving only a lateral streaming flow $(0, V, 0)$, and in this respect it is identical to the non-lifting problem considered in §§2–4. However, the significant difference between the lifting and non-lifting problems is the end-condition which must be imposed at the trailing edge. The condition (4.14) is now appropriate only at the leading edge, and must be replaced at the trailing edge by a

suitable Kutta condition,† stating that the longitudinal velocity component is continuous at the trailing edge. Thus, noting the relation (4.10) for the longitudinal component of the inner velocity field, we replace (4.14) by the new end conditions,

$$U(x)C(x) = 0 \quad \text{at} \quad x = -1 \quad \text{(leading edge)} \tag{7.1}$$

and

$$(UC)' = 0 \quad \text{at} \quad x = 1 \quad \text{(trailing edge)}. \tag{7.2}$$

The matching procedure leading to (4.13) is unchanged in the present case, but now the constant $P(0)$ in (4.13) must be chosen to satisfy the Kutta condition, in a manner which is familiar from the linearized theory of two-dimensional wings. Thus it follows that

$$P(0) = -V + \frac{1}{\pi}\int_{-1}^{1} U(\xi)\left(\frac{1+\xi}{1-\xi}\right)^{\frac{1}{2}} d\xi, \tag{7.3}$$

and (4.13) then assumes the form,

$$(UC)' = -\frac{1}{\pi}\left(\frac{1-x}{1+x}\right)^{\frac{1}{2}}\int_{-1}^{1}\left(\frac{1+\xi}{1-\xi}\right)^{\frac{1}{2}}\frac{U(\xi)\,d\xi}{\xi-x} + V\left(\frac{1-x}{1+x}\right)^{\frac{1}{2}}. \tag{7.4}$$

The lifting-line integral equation (4.19) is valid without modification, but (4.17) must be replaced, using (4.15) and (7.3), by

$$U(x)C(x) = -\frac{1}{\pi}\int_{-1}^{1} U(\xi)K(x,\xi)\,d\xi + V(1-x^2)^{\frac{1}{2}} - P(0)(\tfrac{1}{2}\pi + \sin^{-1}x). \tag{7.5}$$

The first term in an iterative solution, for large values of the blockage parameter C, or small values of the wall separation a, is

$$U(x) \cong (V/C)[(1-x^2)^{\frac{1}{2}} + \tfrac{1}{2}\pi + \sin^{-1}x]. \tag{7.6}$$

The opposite extreme of small C, or large wall-separation, gives the limiting solution $U = V$ which can be readily confirmed from (7.5).

Now let us consider the lift force parallel to the y axis and the moment M about the z axis, which are analogous to the usual aerodynamic lift and pitching moment. A convenient approach is that of Lighthill (1960), who showed that the longitudinal distribution of the lift force can be expressed in terms of the sectional added-mass coefficient.‡ Thus, in the present notation, the lift-force distribution is given by the expression

$$l(x) = V\frac{d}{dx}m_{yy}, \tag{7.7}$$

where m_{yy} is the sectional added-mass force, which may be obtained in the blocked three-dimensional flow from (5.3). Thus, combining (5.3) and (7.7), it follows that

$$l(x) = \frac{d}{dx}[-\rho V S(x) + 2\rho a U(x)C(x)]. \tag{7.8}$$

† A Kutta condition is not usually imposed in the conventional theory of wings of small aspect ratio. Essentially, the need to impose end conditions, both here and in the non-lifting case of §4, is a consequence of the three-dimensional effects introduced by the walls.

‡ One of the referees has noted that this relationship between the lift force and the added mass was derived and used in several earlier papers, and indeed can be inferred from the original work of Munk. For a more complete discussion of this point, reference can be made to the monograph of Miles (1959).

Integrating with respect to x, we obtain the total lift force

$$L = 2\rho a U(1) C(1) \tag{7.9}$$

and, after a partial integration, the moment

$$M = L + \rho V \mathscr{V} - 2\rho a \int_{-1}^{1} U(x) C(x)\, dx. \tag{7.10}$$

Here $\mathscr{V}$ is the body volume, defined by (5.1); we have used the leading-edge condition (7.1) and the fact that the sectional-area $S(x)$ vanishes at the ends.

In the case of large blockage, (7.6) yields the correct limiting results for a two-dimensional uncambered aerofoil. More generally, the lift can be expressed in terms of the constant $P(0)$, by using the Fredholm equation (7.5) to evaluate (7.9), and it follows that

$$L = -2\pi\rho a P(0), \tag{7.11}$$

or, from (7.3),

$$L = 2\rho a \left\{ \pi V - \int_{-1}^{1} U(x) \left(\frac{1+x}{1-x} \right)^{\frac{1}{2}} dx \right\}. \tag{7.12}$$

Similarly, the moment (7.10) can be obtained by integration of (7.5), in the form

$$M = V(\mathscr{V} - \pi a) + 2\rho a \int_{-1}^{1} U(x)(1-x^2)^{\frac{1}{2}}\, dx. \tag{7.13}$$

The variational technique employed in §5 cannot be applied in a straightforward manner to obtain approximations for the lift and moment, since the parameter $P(0)$ in (7.5) destroys the symmetry of the kernel. This difficulty could presumably be overcome, but for $C(x)$ = constant it is a simple matter to find rational approximations for the lift and moment, analogous to (5.9) and (6.6), simply by finding a rational function which is correct in the limiting cases of large and small C. In this manner, we obtain the approximations,

$$L \cong 2\pi\rho a V \frac{C}{\pi + C} \tag{7.14}$$

and

$$M \cong \rho V \mathscr{V} - 2\pi\rho a V \frac{C}{\pi + 2C}. \tag{7.15}$$

In the case of a rectangular flat plate, the moment is associated entirely with lifting effects, and the centre-of-pressure is situated at the point,

$$x_{cp} = \frac{M}{L} = -\frac{\pi + C}{\pi + 2C}. \tag{7.16}$$

Thus, as might be anticipated, the effects of blockage are to move the centre-of-pressure downstream from the leading edge, and ultimately to the quarter-chord point.

8. Discussion and conclusions

To illustrate the preceding results for the forces and moments associated with added mass and lift, we shall consider the case of a rectangular flat plate, using (3.6) to determine the blockage parameter C. Thus, from (5.5), (6.7), (7.14) and

(7.15), and utilizing a matrix notation for compactness, we obtain the expressions

$$F_i = \tfrac{1}{2}\pi\rho a\alpha_i/(\beta_i^{-1} + \pi/4C) \quad (i = 1, 2, 3, 4). \tag{8.1}$$

Here,

$$F_i = \{M_{yy}, I_{zz}, L, M\}, \tag{8.2}$$

$$\alpha_i = \{2, \tfrac{2}{3}, V, -V\}, \tag{8.3}$$

and

$$\beta_i = \{1, \tfrac{3}{8}, 4, 2\}. \tag{8.4}$$

Substituting for the blockage parameter C, from (3.6), it follows that

$$F_i = \tfrac{1}{2}\pi\rho a\alpha_i\left[\beta_i^{-1} - \frac{\pi^2}{4a\log\cos(\pi d/2a)}\right]^{-1}, \tag{8.5}$$

where d is the span of the plate. In the limit $a \to \infty$, (8.5) reduces to the conventional slender-body results $\frac{1}{4}\pi\rho d^2\alpha_i$. Dividing (8.5) by this limit, we obtain the non-dimensional ratios

$$\frac{F_i(A,\delta)}{F_i(A,0)} = \left[A\delta\beta_i^{-1} - \frac{\pi^2\delta^2}{8\log\cos\frac{1}{2}\pi\delta}\right]^{-1}, \tag{8.6}$$

where $A = \frac{1}{2}d$ is the aspect ratio of the plate, and $\delta = d/a$ is the blockage ratio between the span of the plate and the separation of the walls. In the limit of fully blocked flow, $\delta = 1$, the two-dimensional results are recovered in the form,

$$\frac{F_i(A,1)}{F_i(0,1)} = \frac{\beta_i}{A}. \tag{8.7}$$

The ratios (8.6) indicate the relative amount by which the four forces and moments are increased as a result of the walls. These ratios are displayed graphically in figure 4, plotted against the parameter δ. The three curves shown are for differing values of the ratio A/β_i, which can be related to the aspect ratio of the plate for each of the four forces and moments, by noting the appropriate value of the constant β_i from (8.4). It is clear that blockage due to wall effects is most significant in the case of the lift force, and least important for the added-moment-of-inertia. In general, however, the wall effects are very weak until the blockage ratio exceeds one-half, and it must exceed 0·9 in order for the forces and moments to be doubled relative to their original values. We emphasize that these results are only approximate, since they were not obtained from the exact solutions of the appropriate integral equations; but for one case (the virtual mass force), where Glauert's solution is available for comparison, it is known that the maximum error incurred by our approximation is 5 %. Moreover, the fundamental limitations of small aspect ratio and wall separation must be borne in mind, as these were the basic assumptions of our analysis. With respect to the wall separation, we have already noted that the final results are correct in the limit of infinite wall separation, so that the limitation of small wall separation may be regarded as unimportant. Strictly speaking, however, while the limiting values of the forces are correct, as $a \to \infty$, the curves in figure 4 are not in accordance with the proper behaviour at large values of the parameter a, or small values of δ. In fact, the derivatives of (8.5) and (8.6) with respect to δ, evaluated at $\delta = 0$, are negative, indicating a predicted *decrease* in the forces and moments due to block-

age. (The magnitude of this decrease is so small that it does not appear in the graphs; for $A = 0{\cdot}2\beta_i$ the minimum value of the ratio (8.6) is about 0·98.) This decrease is contradicted by physical intuition; moreover, the appropriate approximations for $a \gg 1$ can be readily developed, e.g. by consideration of the upwash induced at large distances from a low-aspect-ratio foil; it follows that there will be an *increase* in the lift which is $O(1/a)$.

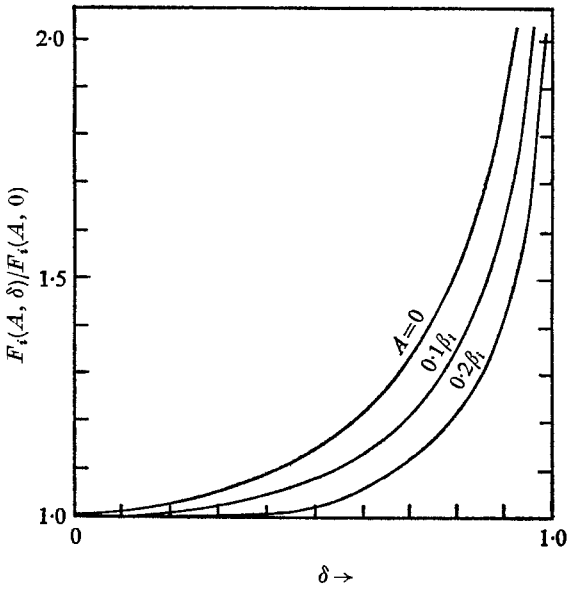

FIGURE 4. The effect of walls on the added-mass force and moment and the lift force and moment, for a rectangular flat plate of small aspect ratio which is oriented with its short sides normal to the walls. The abscissa is the blockage ratio d/a, where d is the length of the short sides of the plate and a is the width between the walls. $A = \frac{1}{2}d$ is the aspect ratio and the four constants $\beta_i = \{1, \frac{3}{8}, 4, 2\}$ correspond to the added-mass force, added moment of inertia, lift force, and lift moment, respectively.

With respect to the manoeuvring of ships, it is apparent that the effects of shallow water will be negligible unless the ship's draft is substantially greater than half of the water depth but, before making definite statements, one should account for the thickness effects resulting from the fullness of the ship, which will affect the added mass and moment, and the lift moment, but not the lift force. Some support for these statements is provided by the recent experiments reported by Norrbin (1969). The experimental facility consists of a towing tank, which is specifically constructed for performing tests with ship models in shallow water; the length and width of the channel are 140 m and 10 m, respectively, and the water depth is variable. In this facility, a model of a large tanker was towed at small yaw angles, and the resulting side force and moment were measured. The model was propelled by its own propeller, and run at a Froude number of 0·078 based upon its length; at such a low Froude number, it may be presumed that free-surface effects will be minimal. The length and draft of the model were 3·614 m and 0·165 m, so that the effective aspect ratio is 0·092.

Table 1 shows values of the experimental force and moment coefficients, for two different water depths, and corresponding predictions from (8.5).

$\delta = d/a$	$C_{L\alpha} = \dfrac{2L}{\frac{1}{2}\rho V^2 \alpha L_s d}$		$C_{M\alpha} = \dfrac{2M}{\frac{1}{2}\rho V^2 \alpha L_s^2 d}$	
	(Experiment)	(Theory)	(Experiment)	(Theory)
0·158	0·248	0·145	0·110	0·0722
0·774	0·365	0·202	0·428	0·0975
Ratio:	1·47	1·40	3·89	1·35

TABLE 1. Comparison between experimental and theoretical coefficients of lift force and moment for a yawed ship model, for depths of water $\frac{1}{2}a = \frac{1}{2}d/\delta$. The ship's velocity is here denoted by V, yaw angle by α, length by L_s, and draft by $\frac{1}{2}d$. L and M are the lift force and moment acting on the hull. The third line in the table shows the ratio of the corresponding coefficient for each of the two depths, and is comparable to the ratio plotted in figure 4.

It is apparent from table 1 that the theoretical and experimental values of the lift force and moment are substantially different. However, the third line of the table shows the relative increase in each force or moment due to the shallow water, and in this respect alone there is satisfactory agreement between theory and experiment for the lift force.

For the lift force, it is likely that the absolute differences between theory and experiment are due primarily to viscous effects, notably separation near the stern, and to the stabilizing effect of the ship's propeller and rudder. Indeed, for deep water it is well known that the classical slender-body theory generally underestimates the observed side force acting on a yawed ship hull. Similar remarks apply also to the moment, but here, in addition, the theoretical prediction has been made without including thickness effects. Thickness effects can be included in the computations, as indicated by (7.15), but this requires a numerical solution for the two-dimensional blockage parameter $C(x)$, which will depend on the detailed shape of the ship hull and on the depth of water. Preliminary computations for a rectangular profile indicate substantially greater shallow-water effects; taking a rectangle having the same area as the mean sectional area of the above-mentioned tanker model, and the same draft, and setting $\delta = 0{\cdot}774$, we find that the two-dimensional added-mass coefficient is increased by a factor of 4·8 with respect to its deep-water value. Since the corresponding result for the flat plate is a factor of 1·4, it is clear that thickness effects must be included in any realistic estimation of the lift moment acting on a yawed ship hull.

The work was supported by the Office of Naval Research, Contract N00014-67-A-0204-0023. I am indebted to Dr E. O. Tuck of the University of Adelaide for bringing the problem to my attention, and for a stimulating discussion of the method of solution. I also thank Mr Nils Norrbin of the Statens Skeppsprovningsanstalt, Göteborg, for providing the experimental data listed in table 1.

REFERENCES

GLAUERT, H. 1948 *The Elements of Aerofoil and Airscrew Theory* (second edition). Cambridge University Press.

LAMB, H. 1932 *Hydrodynamics*. New York: Dover.

LIGHTHILL, M. J. 1960 Note on the swimming of slender fish. *J. Fluid Mech.* **9**, 305–317.

MILES, J. W. 1959 *The Potential Theory of Unsteady Supersonic Flow*. Cambridge University Press.

MILES, J. W. 1967 Surface-wave scattering matrix for a shelf. *J. Fluid Mech.* **28**, 755–767.

MUSKHELISHVILI, N. I. 1946 *Singular Integral Equations* (second edition). Moscow. (English translation, 1953. Groningen: P. Noordhoff N.V.)

NEWMAN, J. N. 1965 The force and moment on a slender body of revolution moving near a wall. *David Taylor Model Basin Report* no. 2127.

NORRBIN, N. H. 1969 Analytical modelling and experimental results for confined water tanker manoeuvring. *Statens Skeppsprovningsanstalt* Publication no. 67.

SEDOV, L. I. 1950 *Two-Dimensional Problems in Hydrodynamics and Aerodynamics*. Moscow–Leningrad. (English translation, 1965. New York: Interscience.)

THWAITES, B. (ed.) 1960 *Incompressible Aerodynamics*. Oxford: Clarendon Press.

TUCK, E. O. 1966 Shallow-water flows past slender bodies. *J. Fluid Mech.* **26**, 81–96.

VAN DYKE, M. D. 1964 *Perturbation Methods in Fluid Mechanics*. New York: Academic.